Understanding the Evolution of Luminescent Gold Quantum Clusters in Protein Templates

Kamalesh Chaudhari,[†,‡] Paulrajpillai Lourdu Xavier,[‡] and Thalappil Pradeep[‡,*]

[†]Department of Biotechnology and [‡]DST Unit of Nanoscience (DST UNS), Department of Chemistry, Indian Institute of Technology Madras, Chennai 600 036, India

ABSTRACT We show that the time-dependent biomineralization of Au^{3+} by native lactoferrin (NLf) and bovine serum albumin (BSA) resulting in near-infrared (NIR) luminescent gold quantum clusters (QCs) occurs through a protein-bound Au^{1+} intermediate and subsequent emergence of free protein.

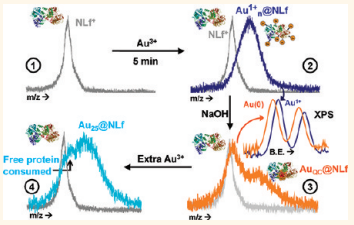

The evolution was probed by diverse tools, principally, using matrix-assisted laser desorption ionization mass spectrometry (MALDI MS), X-ray photoelectron spectroscopy (XPS), and photoluminescence spectroscopy (PL). The importance of alkaline pH in the formation of clusters was probed. At neutral pH, a Au^{1+}—protein complex was formed (starting from Au^{3+}) with the binding of 13—14 gold atoms per protein. When the pH was increased above 12, these bound gold ions were further reduced to Au(0) and nucleation and growth of cluster commenced, which was corroborated by the beginning of emission; at this point, the number of gold atoms per protein was ~25, suggesting the formation of Au_{25}. During the cluster evolution, at certain time intervals, for specific molar ratios of gold and protein, occurrence of free protein was noticed in the mass spectra, suggesting a mixture of products and gold ion redistribution. By providing gold ions at specific time of the reaction, monodispersed clusters with enhanced luminescence could be obtained, and the available quantity of free protein could be utilized efficiently. Monodispersed clusters would be useful in obtaining single crystals of protein-protected noble metal quantum clusters where homogeneity of the system is of primary concern.

KEYWORDS: quantum clusters · proteins · biomineralization · luminescence · cluster evolution

Quantum clusters (QCs) of noble metals showing intense photoluminescence belong to new class of materials.[1−6] Understanding the structural evolution of clusters is central to understanding their properties. Multitude of techniques have been applied to study clusters in general.[7−11] Recent studies involve understanding of geometric and electronic structure, chirality, and photophysics using a host of tools such as X-ray crystallography,[12] advanced theoretical methods, high-angle annular dark-field scanning transmission electron microscopy (HAADF-STEM),[13] and circular dichroism spectroscopy (CD). Among the various techniques, mass spectrometry has been an indispensable technique in characterizing quantum clusters.[1,14] Electrospray ionization mass spectrometry (ESI-MS) has been particularly useful to characterize monolayer-protected gold and silver clusters.[1−6,15−17] Dharmaratne *et al.* have demonstrated the use of matrix-assisted laser desorption and ionization mass spectrometry (MALDI MS) for studying time-dependent size evolution of quantum-confined thiolate-protected Au_{25} clusters.[18] Other techniques such as *in situ* X-ray absorption fine structure (XAFS) spectroscopy have also been utilized to study the structural evolution of medium-sized gold clusters[19] and initial nucleation mechanism of gold nanocrystals of less than 1 nm core size.[20]

A recent addition to the family of QCs is their protein-protected analogues. Myriad of inorganic nanomaterials and nanostructures have been formed by biomineralization or biomimetic mineralization in natural and synthetic polymers like peptides, nucleotide sequences, proteins, and dendrimers.[3,21−24] However, luminescent noble metal QCs in proteins are a new class of materials. Apart from bovine serum albumin (BSA),[22,24] we had demonstrated the possibility of utilizing multifunctional transferrin proteins, having potential biomedical applications, such as lactoferrin (Lf), a milk transferrin for cluster synthesis, and shown the potential applications of such protein-protected clusters.[23−28] Recently, Schneider's group has synthesized gold clusters in human serum transferrin,[29] a structural analogue of Lf.[30] Formation of quantum-confined gold clusters of subnanometer dimensions in proteins is intriguing from the point of view of biomineralization. Understanding the biomineralization process provides important information about nature's ways to form distinct but complex inorganic structures, and this knowledge can be utilized to synthesize nanomaterials

* Address correspondence to pradeep@iitm.ac.in.

Received for review July 31, 2011 and accepted October 19, 2011.

Published online October 19, 2011
10.1021/nn202901a

by green synthetic methods which are closer to natural methods and, therefore, better useful in, but not limited to, biology.[3,21−34] Biomineralization processes are directed by specialized biomolecules like proteins, DNA, *etc.* in living organisms which can be mimicked *in vitro* to synthesize materials of interest, and these processes remain topics of hot debate.[3,21−34] A recent study by Yi Lu and group has shown that single crystals of lysozyme can be used to study the time-dependent, protein-directed growth of nanometer-sized plasmonic gold nanoparticles (GNP) in a static environment.[34]

In the present work, we have used MALDI MS to probe the time-dependent size evolution of QCs formed by the biomineralization of Au^{3+} directed by proteins Lf and BSA in aqueous reaction mixtures. Unlike the single crystals of protein used to study the growth of GNPs,[34] here the environment is highly dynamic. It has been shown that solution-state and solid-state protein structures differ because of the presence of flexible domains inside the protein.[35,36] Hence it is important to study cluster growth in the solution phase which allows substantial structural relaxation. The protein selected for this study, lactoferrin (also called as lactotransferrin), has been reported as a structurally flexible protein.[37] We used native lactoferrin (NLf) in this study. It is an iron binding glycoprotein with the molecular weight of ~83 kDa. Lf contains 33 cysteine, 21 tyrosine, and 9 histidine residues.[38] It has been reported that tyrosine residues can reduce Au^{3+} at pH above 10 (pK_a of Tyr) and cysteine can bind to reduced gold to stabilize clusters inside the protein.[22,23] It has been also shown that nucleation of gold atoms to form clusters inside the single protein crystals can be also be facilitated by histidine residues.[34] Our study gives insights into the mechanism of the formation of subnanometer-sized clusters in proteins which is, eventually, a biomineralization process and demonstrates the important role of mass spectrometry in studying Au_{QC} systems. We have monitored growth of clusters in different molar ratio combinations of Au^{3+}/NLf in which NLf concentration was kept constant and Au^{3+} concentration was varied from 0.5 to 4.5 mM in steps of 1 mM. It gives comprehensive information about changes occurring in the growth process and major emissive structures formed as a function of time. Monodispersity and control over cluster synthesis are mandatory for crystallization, especially in the case of drug delivery and catalysis.[39−41] Our study suggests possible ways to control properties such as luminescence and monodispersity. These extensive studies with mass spectrometry are especially difficult as reproducible and reliable mass spectra of such systems require careful optimization. To the best of our knowledge, this is the first time such studies have been conducted.

RESULTS AND DISCUSSION

Synthesis and physicochemical characterization of gold clusters in lactoferrin (Au_{QC}@NLf) were reported from our group.[23] Briefly, synthesis involves incubating the protein with Au^{3+} at alkaline pH[22] (see Materials and Methods). Optimum molar ratio of Au^{3+}/NLf for cluster growth is nearly 17:1 (150 μM NLf and 2.5 mM Au^{3+}). Parent protein shows a downward shift in mass by ~600 Da at alkaline pH compared to the protein in the native state (Figure 1 and Supporting Information, Figure S1). This downshift was found to be irreversible when pH was reverted to neutral by the addition of HCl (experimental details are given in Supporting Information). As it is known, all of the disulfide bonds break at high alkaline pH. We believe that this mass shift may be closely associated with breaking of the disulfide bonds and concomitant effects. Another possibility may be the increased deamidation at elevated pH.[42]

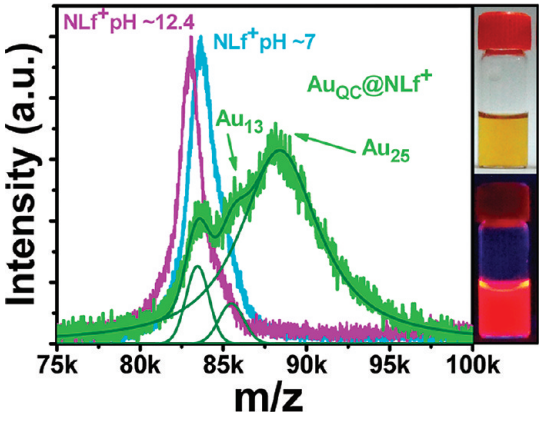

Figure 1. MALDI MS data of NLf at pH ~7, NLf at pH ~12.4, and Au_{QC}@NLf prepared at pH ~12.4 showing the presence of Au_{13} and Au_{25} cores. Photographs on the right are cluster solutions taken in visible (top) and UV (bottom) light.

The mass spectrum of Au_{QC}@NLf suggested the presence of Au_{25} and Au_{13} clusters apart from the free protein, and the quantity of the former was higher than the latter. From the mass spectral intensities, and assuming all of the parameters affecting mass spectral intensity are the same, ~88.82% of the clusters are in the Au_{25} form and the rest of the contributions are due to Au_{13} (4.04%) and NLf (7.14%).

The distribution of ~Au_{25} is approximately three times larger than the distribution of ~Au_{13} as shown from the full width at half-maximum (Supporting Information, Table 1). These clusters emit in the NIR region (615−715 nm), which is the characteristic emission range of Au_{23} and Au_{25} clusters.[43] Au_{QC}@NLf shows two excitation maxima at ~370 and ~510 nm for the emission maximum at ~665 nm, while the protein alone shows excitation at 340 nm (em = 440 nm).[44−46] Spectral overlap of NLf emission with Au_{QC}@NLf excitation indicates that there is Förster resonance energy transfer (FRET) occurring between NLf and Au_{QC}@NLf.[23] Emission of clusters show a red shift upon increase in pH.[23] As it is known from a number of detailed studies, MS of protein-bound clusters is complex and difficult. The mass loss of 600 Da and necessity of this in the cluster formation are important aspects of study. Definitive answers for

these are under investigation. Further, the lower *m/z* region of the spectra is complex with several features and does not show cluster features. However, the higher *m/z* region is distinct with molecular ion signature. In view of this, we focused on this region alone to understand the evolution of clusters.

Size Evolution of Au_{QC}@NLf. To understand how Au^{3+} ions bind to protein and how it leads to the formation of two different clusters as time progresses, we have monitored concentration and time-dependent evolution of gold clusters using MALDI MS and photoluminescence spectroscopy (PL). Initially, growth was monitored for a molar ratio of Au^{3+}/NLf (17:1). NLf concentration was kept constant throughout this study at 150 μM, and only Au^{3+} concentration was changed wherever required to study concentration dependence. Then samples were collected from the reaction mixture under continuous stirring condition at intervals and spotted for MALDI MS, and the droplets were dried in ambient air and examined. Since the parent protein shows a slight shift in mass upon change in pH (Figure 1), shift in mass of the cluster system was compared against the mass of NLf at pH ~12.4 (Figure 2). At the beginning of the reaction, NLf picks up Au^{3+} (biomineralization) immediately upon exposure. The ions may bind to different amino acid residues (histidine, tyrosine, serine, arginine, asparagine, and threonine) present in the protein that are expected to interact with gold ions. Static state single-crystal study has suggested that this binding can be facilitated by ε-N of histidine-15 and tyrosine-23 residues of lysozyme, where the time scale of growth of the gold nanoparticle was slow because the protein was structurally undisturbed in the crystal lattice.[34] In our study, faster growth is feasible because of structural flexibility, fast kinetics, and dynamic environment in the alkaline pH. Au^{3+} ions bind to NLf as soon as they are added to the protein solution. All of the protein molecules in the system exhibited different extent of uptake, which can be seen by the spread of the mass spectrum (Figure 2), and it was concluded that only negligible amount of free protein exists in the solution, as seen by the poor overlap of the parent protein peak with the tail of the metalated protein peak at ~83 kDa.

Hence it appears that, after picking up most of the Au^{3+} at the beginning of the reaction, cluster nucleation begins after 4 h and leads to the formation of Au_{25} clusters, as proven by PL in the NIR region (Supporting Information, Figures S2–S4); then at 12 h, the presence of smaller sized clusters (Au_{13}) can be seen along with the emergence of a significant parent protein peak in the mass spectrum. As time progressed, an increase in the amount of free protein was observed. In the next section of this paper, we have demonstrated that the observed free proteins at this stage can again be used to make clusters if gold ions are supplied again. This leads to enhanced luminescence. By this two-step

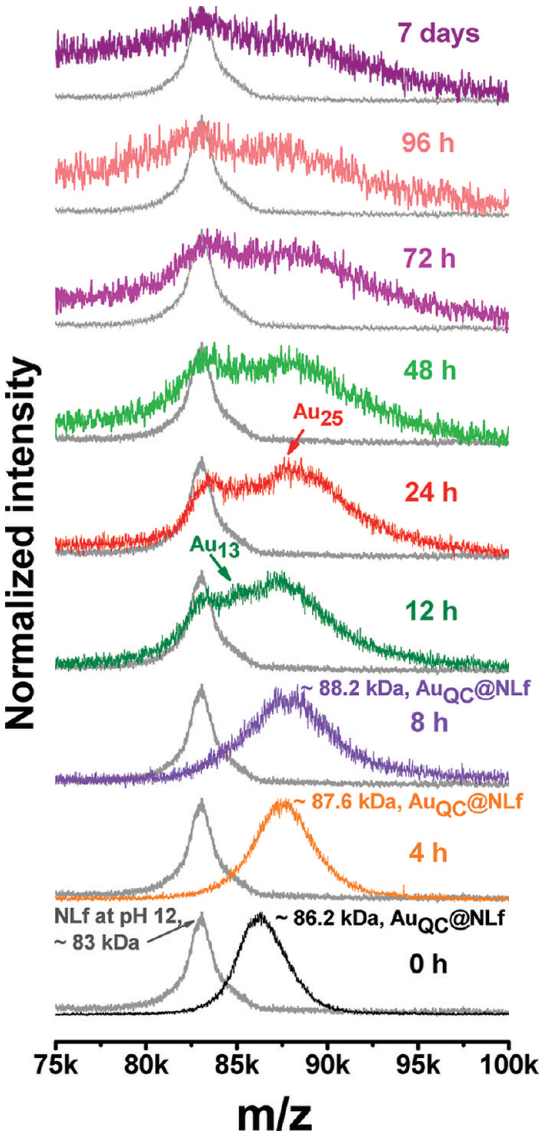

Figure 2. MALDI MS data of Au_{QC}@NLf monitored with time. Reaction was carried out with 150 μM NLf and 2.5 mM Au^{3+} at pH ~12.4 (5% NaOH v/v). Shift in mass was compared against the mass of NLf at pH ~12.4.

synthesis procedure, we can efficiently utilize all of the available protein to synthesize luminescent clusters.

There is a distinct possibility that multiple proteins may bind to a given cluster, but this possibility is unlikely in view of the several-fold reduced size of cluster (less than 1 nm) in comparison to protein (13.89 × 8.7 × 7.34 nm).[47] Nevertheless, to check the likelihood of multiple protein binding, we show a comparison of the monomer and the dimer regions of the protein MS, in Supporting Information, Figure S5. The dimer peak is weak in comparison to the monomer. Dimers of proteins are known to occur naturally and are formed by protein–protein interactions and salt bridges in solution in trace quantities.[48] Both the protein and its dimer form are observable, and both manifest distinct gold uptake peaks at 0 h of exposure. In view of the equal probability of Au^{1+} uptake by both the units of the

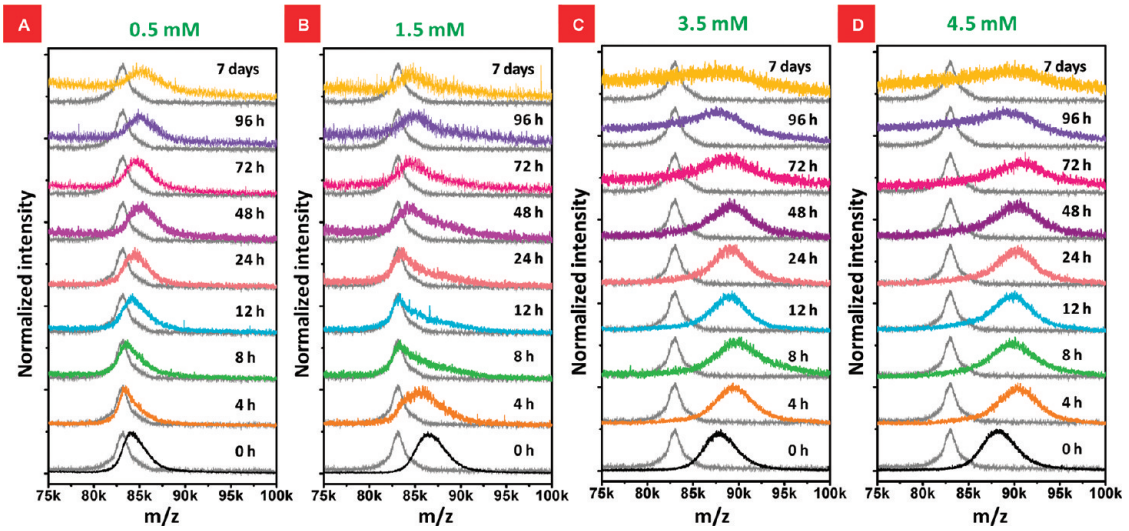

Figure 3. Concentration-dependent size evolution of Au_{QC}@NLf. NLf concentration was kept constant (150 μM), and Au^{3+} concentration was varied from 0.5 mM (A), 1.5 mM (B), 3.5 mM (C), to 4.5 mM (D), and time-dependent MALDI MS data were collected for each concentration, separately.

dimer, MS shows a shift which is ~2 times of the monomer. Upon incubation for 12 h, parent protein is regenerated as expected along with the occurrence of the clusters, Au_{13} and Au_{25}, in the monomer region. In the dimer region, there are several possibilities, such as free dimer devoid of cluster, both units with Au_{25} or Au_{13}, one free unit and the other with Au_{13} or Au_{25}, and one unit with Au_{13} and the other with Au_{25}. All of these possibilities result in a broad convolution which is evident in the spectrum. It is clear that the spectrum is not due to only the 13 and 25 atom bound dimer. It is important to note that a larger cluster containing more numbers of Au atoms bound by multiple proteins does not get nucleated, as it would have resulted in a red-shifted luminescence in view of larger size. The uptake of double the number of gold atoms, its partitioning between the protein units, and the absence of a large red-shifted luminescence (Supporting Information, Figures S2–S4) suggest that smaller clusters are nucleating in single protein units. Absence of free cluster or cluster containing fragments unlike in the case of monolayer-protected clusters also substantiates this proposal, as a cluster bound with several proteins would have resulted in cluster containing fragments, typically Au_nS_m.[43] In addition, DLS data of several other groups indicate the absence of protein aggregates and the presence of monomers after cluster formation, which also implies that these clusters are present in single protein molecules.[22,29]

Concentration Dependence of the Size Evolution of Au_{QC}@NLf. To check whether the occurrence of free protein after a few hours of reaction takes place at higher concentrations of Au^{3+}, too, and to study how Au^{3+} is distributed among the protein molecules so that some protein molecules appear free as time progresses, we have monitored concentration-dependent cluster growth (Figure 3). The data presented show that there are two regimes of Au^{3+} concentrations (Figure 3). In the regime of lower concentration (<2.5 mM, Figure 3A,B), cluster nucleates slowly, and at larger concentration (>2.5 mM, Figure 3C,D), regime-diverse bigger clusters are formed. The macromolecular dynamics and reduction chemistry in the two regimes appear to be distinctly different as evidenced by the slow reduction and formation of clusters. Rising baseline at longer times can be understood on the basis of changes in pH and catalytic activity of quantum clusters. Fragmentation of protein can occur when pH of the environment changes drastically. Also, small clusters, in general, participate in oxidative catalysis, and several studies exist on this. As a result, selective activation of chemical bonds is likely, which could lead to fragmentation and rising baseline. The appearance of free protein suggests the release of gold from its protein-bound state. From an understanding of aurophilic interactions in Au^{1+} systems[49] (see below for data on the existence of Au^{1+}), we infer that slow intermolecular transfer of metal is feasible. As the nucleation of nanoparticles from Au^{1+} thiolates has been demonstrated earlier[34] and in conjunction with the observation of transfer of metal atoms in the growth of gold nanoparticle in lysozyme,[34] we conclude that such gold transfer inferred here is likely. Samples were monitored up to seven days for all of the concentrations and up to three months for the optimized concentration (2.5 mM) (Supporting Information, Figure S6).

After 48 h, no considerable change was observed in the mass spectra. As far as the 0 h mass spectrum was concerned, all of the gold available was distributed among the available protein molecules. As a result, beyond a certain concentration of Au^{3+}, no large shift is seen in the mass spectra (Supporting Information, Figure S7). This shows that instantaneous binding

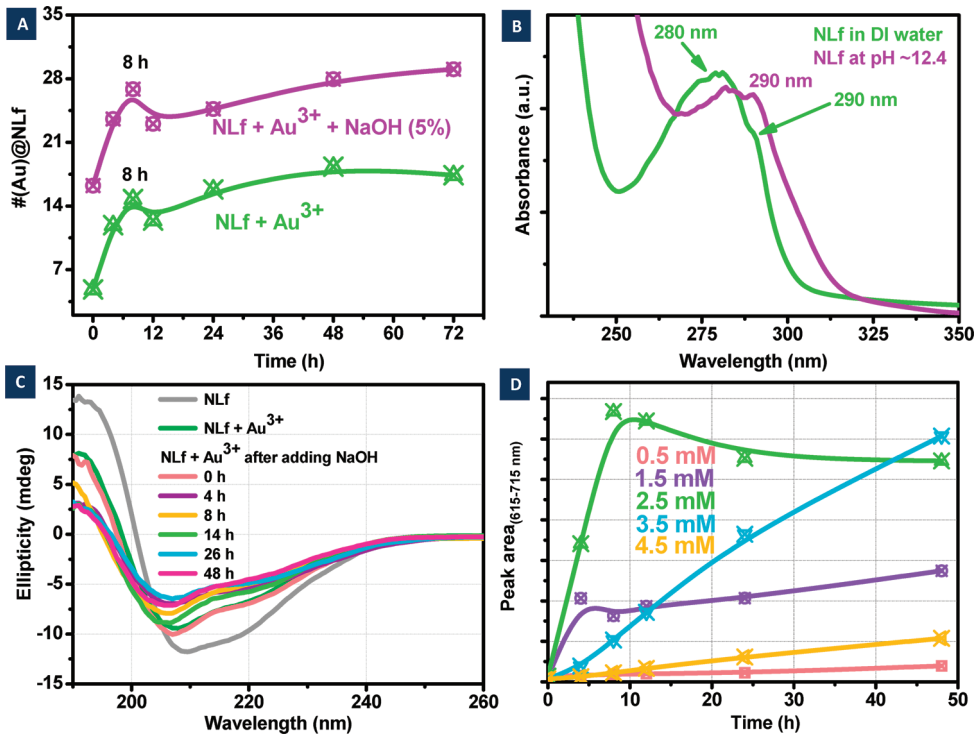

Figure 4. (A) Number of gold atoms (#(Au)@NLf) held by NLf plotted against time, in the presence and absence of NaOH. Reaction was carried out with 17:1 molar ratio of Au^{3+}/NLf, and 5% NaOH (v/v) was added to synthesize the clusters. (B) UV−vis spectrum of NLf in DI water and at basic pH (~12.4), indicating conformational changes of protein at alkaline pH. (C) Circular dichroism spectra of Au_{QC}@NLf monitored with time. Reaction was carried out with 150 μM NLf and 2.5 mM Au^{3+} at pH ~12.4 (5% NaOH v/v). (D) Variation in the integrated area of emission from 615 to 715 nm during cluster growth at various Au^{3+} concentrations, keeping NLf concentration the same.

occurs at available sites and more incorporation of gold per protein is impossible.

Role of NaOH in the Synthesis of Au_{QC}@NLf. Since these clusters were formed only at basic pH, we have investigated the role of NaOH in the synthesis. MALDI MS, PL, and XPS studies were done in the presence and absence of NaOH. Peak difference between Au_{QC}@NLf and NLf (at pH 12.4) was calculated from MALDI MS studies, which revealed changes in the number of gold atoms held by NLf (#(Au)@NLf) with time. In the absence of NaOH, #(Au)@NLf does not increase beyond 15 because no nucleation of clusters began (Figure 4A). This was supported by the luminescence data, as well (Supporting Information, Figure S8).

In the absence of NaOH, at 0 h, #(Au)@NLf was 4−5, which quickly increased to ~13 (the inner core of Au_{25}).[1] Longer term probing showed that, in the absence of NaOH, #(Au)@NLf was stable around 14−15 and no emergence of free protein was seen (Supporting Information, Figure S9). However, in the presence of NaOH, #(Au)@NLf increases up to ~28 along with the occurrence of free protein (Figure 2 and Figure 4A). As soon as NaOH was added to the solution, the pH of the solution increased up to ~12.4, which is higher than the pK_a values (7.4−9.1)[50] of cysteine thiols (33 cysteine residues per NLf molecule) in proteins.

Occurrence of free protein and increase in the #(Au)@NLf happens only after addition of NaOH and suggests an interprotein gold ion transfer, a possible mechanism in which the NLf molecules, which have started cluster nucleation, attract gold held by other protein molecules. The possible reason for this may be aurophilicity, which is preferential attraction of atomic entities to aggregate around nucleation sites and arises mainly due to the relativistic expansion of the gold d orbitals.[49,51,52] Along with this, the structural and electronic stability provided by Au_{25} may be also reason for this redistribution of gold ions.[1] For the above-discussed formation of gold cluster and redistribution of gold ions between proteins, the conformation of the protein must undergo a certain degree of changes to facilitate the effective formation of clusters.[23] UV−vis spectroscopic analysis of tryptophan absorption[53] and CD spectroscopic analysis of secondary structure revealed that protein's secondary structure changes with time (Figure 4B,C). To verify such changes, we have monitored circular dichroism spectra of Au_{QC}@NLf with time. Changes in secondary structure of the protein were found as a function of incubation time under the experimental conditions (Figure 4C). The valleys at 208 and 222 nm indicate presence of α-helical structures.[23] As time passes, the valley at 208 nm shows a blue shift and the valley at 222 nm becomes shallower due to emergence of random coiled structures. The data suggest that unfolding of protein with time facilitates formation of the clusters.

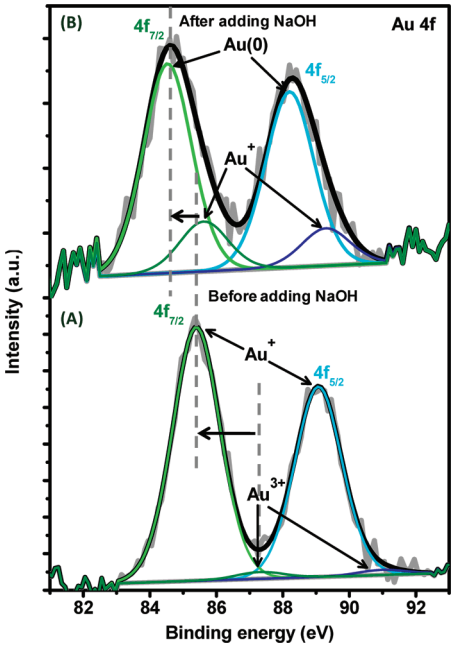

Figure 5. X-ray photoelectron spectra of NLf and Au^{1+} conjugate in the (A) absence and (B) presence of NaOH after 5 min of reaction. Individual components are fitted.

XPS studies have shown that, in the absence of NaOH, protein reduces most of the Au^{3+} to Au^{1+} and forms a complex (Figure 5). The Au $4f_{7/2}$ binding energy of 85.4 eV is due to Au^{1+} and that of 87.3 eV is due to Au^{3+}. XPS curve fitting has shown that only negligible amount of Au^{3+} (2.62%) remained and most of the gold is in Au^{1+} (97.38%) form after 5 min of reaction. In the presence of NaOH, within 5 min, around 80.76% Au^{1+} gets reduced to Au(0) to form clusters and the $4f_{7/2}$ peak appears at 84.5 eV, close to Au(0). Same binding energy value is seen in Au_{QC}@NLf and gold clusters, in general.[22,23]

The remaining 19.24% Au^{1+} can be considered as the gold which gets redistributed among the protein molecules during cluster growth, and after 24 h, less than 10% of Au^{1+} remained, which may be due to smaller clusters or surface atoms of the clusters formed.[2] Hence the study establishes that exposure of Au^{3+} leads to the formation of Au^{1+}–protein complex, and the gradual evolution of the clusters can be attributed to the reduction of Au^{1+}, which takes place when slow unfolding of protein occurs upon the addition of NaOH and amino acids from the inner core of the protein get exposed by the breakage of disulfide bonds (~16 disulfide bonds in single NLf molecule). We have not explored S 2p region (Supporting Information, Figure S10) of the sample because it shows higher binding energy peaks due to sulfate, sulfite, and sulfonate species as a result of X-ray beam induced damage.[23]

Concentration-Dependent Time Evolution of the Luminescence of Au_{QC}@NLf. There are multiple parameters such as pH, particle size, and nature of ligands which can affect the emission peak position of these clusters.[54] As the cluster size increases, red shift in the emission peak is expected. However, when we monitored the luminescence as a function of time, a blue shift was observed with increasing concentration of Au^{3+} against NLf (Supporting Information, Figure S11). It appears that this effect is due to change in pH as mentioned earlier (note that Au^{3+} is added in the form of $HAuCl_4$).[23] An experiment was performed in which pH of the reaction mixture was maintained constant (pH 12.4 ± 0.03) for all of the molar combinations of Au^{3+}/NLf, and a weak blue shift (~10 nm) was observed in the emission peaks (Supporting Information, Figure S12) which can be attributed to varying chemical environment around the cluster. No significant change in the core was observed from MALDI MS data between pH maintained and not maintained samples (Supporting Information, Figure S13). Integrated area method was used to compare the emission of clusters produced by different molar ratio combinations of protein and gold. Area from 615 to 715 nm (665 ± 50 nm) was calculated since 665 nm was found to be the average emission maximum. From the analysis, 17:1 (2.5 mM Au^{3+}) molar ratio combination of Au^{3+}/NLf was found to give the maximum emission in the shortest incubation time (Figure 4D). Slope of the curve of the peak area (615−715 nm) *versus* time changes after 8 h for 2.5 mM Au^{3+} and after 4 h for 1.5 mM Au^{3+}, which is the same time at which changes were observed in the mass spectra also. Hence luminescence spectroscopy supports the free protein observed by MALDI MS and also proves that this change is not due to fragmentation of the protein as a result of laser irradiation during mass spectrometry. At 0.5 mM, the quantity Au^{3+} is not enough to form clusters which can emit in the region of 615−715 nm. For concentrations higher than 2.5 mM of Au^{3+}, the rate of evolution of luminescence is slower. In the case of 4.5 mM Au^{3+}, much less emission occurs which may be due to the formation of larger sized clusters (Supporting Information, Figures S14 and S15), whereas for 1.5 mM, emission is less since the amount of Au^{3+} available is less and only a fewer number of emissive clusters can be formed. This suggests that the supply of a higher concentration of Au^{3+} in the beginning leads to the formation of nonemissive clusters; hence a proper synthetic approach should involve the supply of gold in a controlled manner. However, no separate emission peak was found for Au_{13} or smaller size clusters. Recent report has shown that green emitting Au_{13} clusters, having emission at 510 nm, can also emit in the NIR region[55] with excitations of 360 and 490 nm, which matches with the excitation and emission of Au_{QC}@NLf. Hence in the case of Au_{13}@NLf, even if the ligands and overall chemical environment around the cluster core is

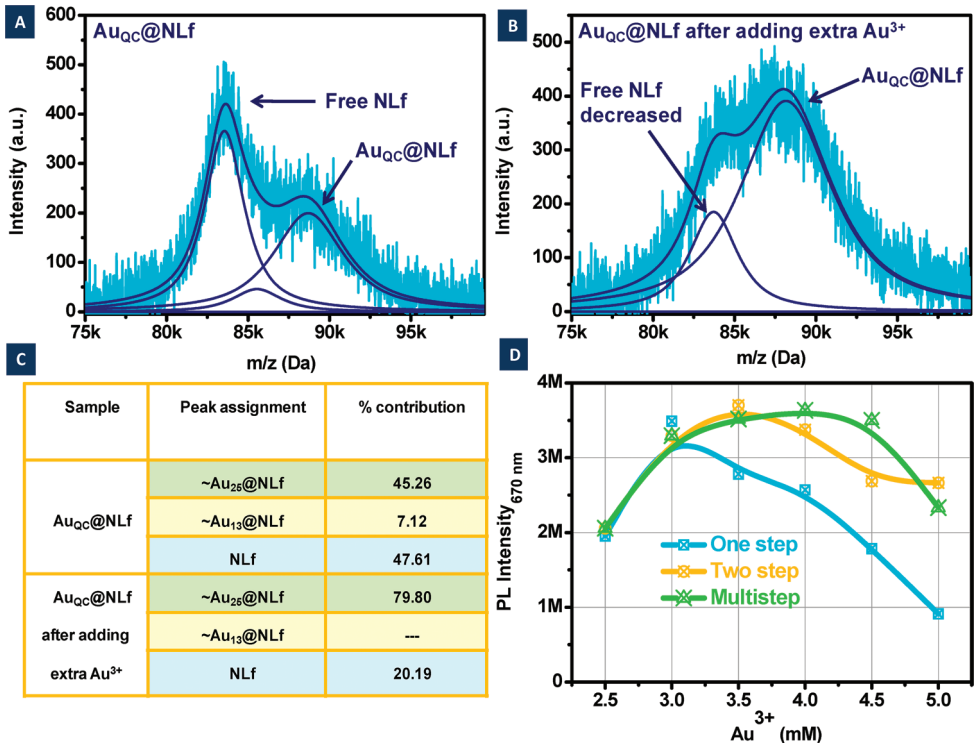

Sample	Peak assignment	% contribution
Au_{QC}@NLf	~Au_{25}@NLf	45.26
	~Au_{13}@NLf	7.12
	NLf	47.61
Au_{QC}@NLf after adding extra Au^{3+}	~Au_{25}@NLf	79.80
	~Au_{13}@NLf	---
	NLf	20.19

Figure 6. (A) MALDI MS data of Au_{QC}@NLf collected after 72 h. (B) MALDI MS data of Au_{QC}@NLf to which extra Au^{3+} was added after 24 h of reaction. Spectrum was collected after 48 h. (C) Table below compares the percentage of Au_{25}@NLf in the reaction mixture. (D) Comparison of the luminescence intensity of the clusters obtained by three different approaches for efficiently utilizing the available amount of protein. Samples were compared according to the final concentration of gold in the reaction mixture.

different, the NIR emitting ability of phosphine-protected Au_{13} observed by Shichibu *et al.*[55] suggests the possible reason for the absence of additional emission peak for Au_{13}@NLf. We have not isolated any Au_{13} intermediate apart from observing in MS data. However, this also suggests another possibility that there may be 13 gold atoms bound to NLf in the ionic form, instead of the quantum cluster form which can be redistributed between protein molecules for Au_{25} formation. Overall luminescence data suggest that rate of evolution is different for different core sizes, but major emissive structures formed were red emitting (Supporting Information, Figures S3 and S4).

Unlike monolayer-protected Au_{25},[43] the protein-stabilized gold quantum clusters have no sharp absorption features in the NIR region, hence we were unable to observe any noticeable change in the absorbance spectra monitored as a function of incubation time. The major peak in the UV−vis spectrum was observed at 280 nm with a shoulder at 290 nm (Figure 4B and Supporting Information, Figure S16). The peak at 280 nm is due to absorption by tyrosine and tryptophan residues in the protein, and the shoulder at 290 nm is due to tryptophan in the polar environment of the protein.[53] This 290 nm feature was found to become prominent when absorbance of NLf was measured at basic pH (~12.4). Multiple features were observed in the wavelength region of 450−800 nm, but no sequential growth pattern or its correlation with other data was seen (Supporting Information, Figure S17).

Development of Different Approaches To Attain Monodispersity of Au_{QC}@NLf. To prove the appearance of free protein during cluster growth, Au_{QC}@NLf was synthesized with the optimized concentration of Au^{3+} (2.5 mM), and after 24 h of reaction, final concentration of Au^{3+} was adjusted in the range of 3−5 mM, which is referred to as a two-step synthesis method (Supporting Information, Scheme 1). About 2-fold increase in the luminescence intensity was observed in this case due to the formation of additional clusters (Supporting Information, Figure S18). Consumption of free protein during the formation of clusters was confirmed by MS (Figure 6A,B). Approximate fitting of the mass spectra has shown that the percentage of Au_{25}@NLf increases after addition of extra Au^{3+} ions and free NLf in the solution decreases (Figure 6C). It has also been shown that the peak appearing for Au_{13}@NLf in the spectrum vanishes after adding extra Au^{3+} ions, which suggests that the reaction intermediate Au_{13} completely turns into Au_{25}.

It was found that increasing the final concentration of Au^{3+} to 3.5 mM is enough for the free protein molecules to interact with excess Au^{3+} to form additional clusters leading to enhanced luminescence (Supporting Information, Figure S18). However, if we increase the final concentration of Au^{3+} more than

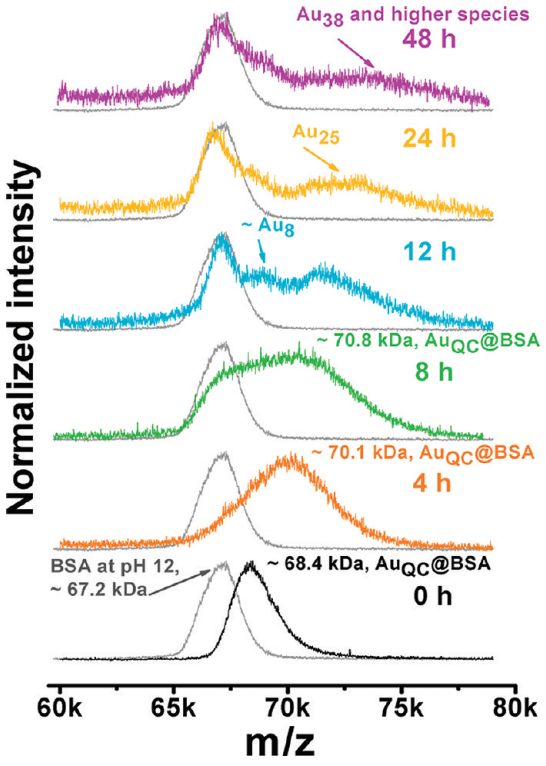

Figure 7. Time-dependent MALDI MS data of Au_{QC}@BSA confirming evolution pattern similar to Au_{QC}@NLf.

3.5 mM, luminescence intensity decreases. As suggested by mass spectra, no bigger size clusters (#(Au) > 25) were formed when the final concentration of Au^{3+} was adjusted to more than 3.5 mM. No noticeable plasmonic features were observed in UV−vis absorption spectra (Supporting Information, Figure S19). Hence reduction in the luminescence intensity is possibly due to quenching by excess gold ions, not due to plasmonic nanoparticles, and may be due to other nonradiative relaxation pathways, mediated by excess gold ions bound to amino acids in the proximity of clusters. To obtain monodispersed clusters, one possibility is to use chromatographic techniques to isolate cluster containing proteins from the mixture of free proteins and proteins with clusters, which is a cumbersome process, since molecular weight difference is less. Here, we have given a simple solution of providing extra gold ions to reduce the quantity of free proteins in the reaction mixture and to convert reaction intermediate Au_{13} to Au_{25} to make the product monodisperse.

To optimize the procedure, three different approaches were used to attain monodispersed clusters with enhanced luminescence (Supporting Information, Scheme 1). These approaches are essentially the same as of the synthesis[22,23] except that extra gold ions were added at specific time intervals for specific molar ratio combination of the reaction mixture. (1) In the one-step approach, gold ions were added in the beginning similar to the reported method[22,23] to make the final concentration of gold in the solution in the range of 2.5 to 5 mM. (2) In the two-step approach, the reaction begins with 17:1 ratio, and after 24 h, extra gold ions were added only once again to make the final concentration of gold between 3 to 5 mM. (3) In the multistep approach, 0.5 mM extra gold ions was added at 24 h time interval four times to make the final concentration 5 mM.

Monodispersed Au_{QC}@NLf was formed for the concentration of Au^{3+} above 2.5 mM when the one-step approach was used and no emergence of free NLf was observed, even after 48 h. However, maximum luminescence intensity was observed when a two-step approach was used for a final concentration of 3.5 mM of Au^{3+} (Figure 6D). Comparison of mass spectra of clusters obtained by one-step and two-step approaches has shown (Supporting Information, Figures S14 and S18) that, in the former, non-emissive bigger size (#(Au) > 25) clusters were formed at higher concentration of Au^{3+} (Supporting Information, Figure S15), but in the two-step synthesis, clusters were of similar size (Au_{25}). Hence, the two-step approach appears to be a more controlled way where free protein efficiently interacts with extra gold ions to form a maximum number of clusters and gives enhanced luminescence as compared to the one-step approach. In the one-step approach, simultaneous availability of a large number of Au^{3+} in the beginning of the reaction leads to the formation of bigger size clusters, but in the two-step approach, Au^{3+} was provided slowly and hence the free protein molecules take them to form clusters. Results of the multistep approach were compared with the other two and were found to be almost similar to the two-step approach (Supporting Information, Figure S20).

Confirmation with Au_{QC}@BSA. To check whether the observed time-dependent evolution of Au_{QC}, especially the occurrence of free protein at specific time points of incubation time, is observable in other Au_{QC}@protein systems also, we probed the evolution of clusters in BSA[22] by MALDI MS (Figure 7). Initially, just after adding Au^{3+}, the mass spectrum shifts completely and no free BSA is seen. After 8 h, smaller size clusters like Au_8 (here alone we see Au_8, but the PL spectral profile for λ_{ex} = 375 and λ_{em} = 450 nm is seen all of the time, even in protein alone) started forming along with the occurrence of free protein, which suggests that this must be a common mechanism of evolution of quantum clusters in protein templates. Other studies such as UV−vis and PL spectroscopy confirmed the mass spectral observations (Supporting Information, Figures S21 and S22). The 440 nm peak[56−58] is due to the intrinsic emission from tryptophan oxidation products of the protein.[23,44−46] Albeit this known fact, we cannot completely rule out the possibility of the presence of smaller blue emitting clusters with the same spectral profile,[59−63] in addition to protein's emission. Smaller blue emitting clusters may be present, and associated charge transfer to bigger clusters may also happen during the formation of larger

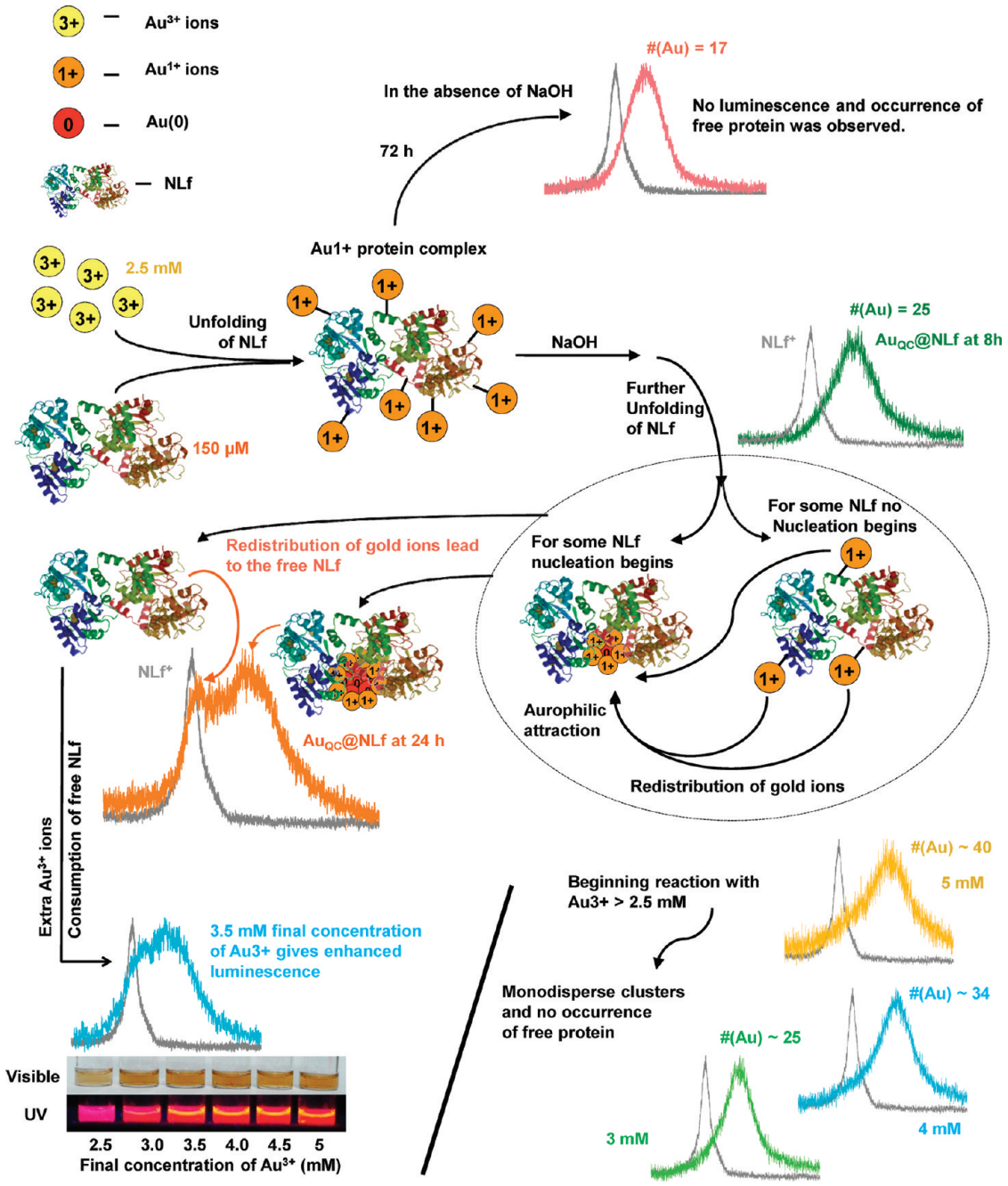

Scheme 1. Observations from the mass spectrometric probing of Au_{QC}@NLf. Steps to achieve monodispersity and enhanced luminescence are also shown.

clusters. However, MS data did not show the presence of such smaller clusters in the Au_{QC}@NLf system. Due to the intrinsic fluorescence of protein at 440 nm, we speculate that major energy transfer happens from protein's intrinsic fluorophores to clusters.

SUMMARY AND CONCLUSIONS

We have probed the evolution of luminescent quantum clusters (QCs) of gold in protein templates in aqueous reaction mixtures having a dynamic environment (Scheme 1). The importance of highly alkaline pH for cluster growth in proteins was studied. We have shown that fast Au^{3+} uptake makes the Au^{1+}-bound protein which gradually incubates clusters in multistep events. Emergence of free protein during cluster synthesis observed at specific time intervals suggests the possibility of redistribution or interprotein transfer of gold ions. We have also observed that addition of extra gold ions at different time intervals to the reaction mixture led to the production of monodispersed clusters with enhanced luminescence. These observations help in synthesizing monodispersed protein-protected clusters and highlight the importance of mass spectrometry in understanding the monodispersity and

evolution of clusters. Synthesis of monodispersed protein-protected quantum clusters is essential for the crystallization of the Au_{QC}@protein system, which is necessary to understand it thoroughly, in answering multifaceted questions related to macromolecule–metal ion interaction and creating tailor-made genetically engineered proteins to form clusters with desired properties. These observations would also be helpful in simulating the formation of gold quantum clusters in biomolecules in aqueous solutions. Along with this, further studies are needed to understand the molecular events involved in interprotein gold transfer and structural changes of protein during cluster growth. It is likely that the cluster formation is highly dependent on the structural properties of a given protein, and we speculate that the mechanism of cluster growth may be different in structurally dissimilar systems.

MATERIALS AND METHODS

Tetrachloroauric acid trihydrate ($HAuCl_4 \cdot 3H_2O$) was purchased from CDH, India. Sodium hydroxide pellets were purchased from Qualigens Pvt. Ltd. Native bovine lactoferrin, ~17.5% iron saturated, purity >96% of Taradon Laboratory was a kind gift from the company Tablets India Pvt Ltd., Chennai, India. Bovine serum albumin was purchased from Fluka. Millipore deionized water (~18.2 MΩ) was used throughout the experiments. Sinapinic acid was purchased from Sigma Aldrich. All chemicals were used as such without further purification.

Synthesis of Au_{QC}@Protein. Au_{QC}@NLf and Au_{QC}@BSA were synthesized as previously described.[22,23] Briefly 1 mL of 5 mM tetrachloroauric acid trihydrate was added to 1 mL of ~300 μM protein (NLf or BSA) solution. After 5 min stirring, 100 μL of 1 M NaOH was added to the mixture and stirred continuously with magnetic stirrer. Samples were collected at subsequent time intervals under continuous stirring and were spotted for MALDI MS analysis. An experiment in which changes in the emission peak position were monitored with time clusters was prepared by the same method as mentioned above, and pH of the sample was adjusted using 1 M NaOH and 1 N HCl to the constant initial value of 12.4 ± 0.03.

Spectroscopic Analysis and Instrumentation. *MALDI MS Analysis.* Sinapinic acid was used as the matrix to enhance ionization. Matrix solution was prepared in a 1:3 mixture of acetonitrile and trifluoroacetic acid (TFA) (0.1% in DI water). At each sampling time, 2 μL of sample was added to 40 μL of matrix solution and mixed with mild sonication for 1 s. Then, 2.5 μL of the resulting mixture was spotted by dried droplet method. An Applied Biosystems Voyager DE Pro MALDI MS instrument was used. A pulsed nitrogen laser of 337 nm was used for ionization. Mass spectra were collected in positive-ion mode and were averaged for 100–250 shots. Spectra collected for Au_{QC}@NLf at optimized concentration (only those which were collected after 24 h) are smoothed using three-point adjacent averaging in Origin software. Shift in mass was compared against the mass of NLf at pH ~12 in the presence of 5% NaOH (v/v). The number of gold atoms held per protein was calculated by

$$(\text{Au})@\text{NLf} = (m/z \text{ value of } Au_{QC}@\text{NLf}^+ - m/z \text{ value of } \text{NLf}^+ \text{at basic pH})/\text{atomic weight of gold}$$

The mass spectrum of Au_{QC}@NLf is fitted with XPSPEAK41 software to determine the fwhm and percentage contribution by NLf and Au_{QC}@NLf approximately.

UV–Vis and Luminescence Spectroscopic analysis. The samples were diluted in DI water, and UV/vis spectra were measured with a Perkin-Elmer Lambda 25 instrument in the range of 200–1100 nm. Luminescence measurements were carried out on a Jobin Vyon NanoLog instrument. The band pass for excitation and emission was set as 3 nm.

X-ray Photoelectron Spectroscopic (XPS) Analysis. XPS analysis was done to confirm reduction of Au^{3+} to form stable clusters. Lyophilized powder of the samples was spotted on carbon tape stuck to the XPS sample plate. XPS measurements were conducted using an Omicron ESCA Probe spectrometer with polychromatic Mg Kα X-rays ($h\nu$ = 1253.6 eV). Curves were fitted and smoothed using CasaXPS software.

Circular Dichroism (CD) Spectroscopic Analysis. Far-UV CD spectrum was obtained using a J-600 spectropolarimeter (JASCO). Then, 0.0125 mg/mL concentration of protein was used in all cases.

Acknowledgment. We thank the Department of Science and Technology, India, for constantly supporting our research on nanomaterials. We thank Taradon Laboratory, Belgium, and Tablets India Pvt. Ltd., Chennai, for their kind gift, lactoferrin. We thank N. Goswami and Prof. S. K. Pal (SNBCBS, Kolkata, India) for CD spectroscopic measurements.

Supporting Information Available: Mass spectrometric and other spectroscopic data under various conditions. This material is available free of charge *via* the Internet at http://pubs.acs.org.

REFERENCES AND NOTES

1. Habeeb Muhammed, M. A.; Pradeep, T. In *Advances in Fluorescence Spectroscopy*; Dushchenkov, A., Ed.; Springer: Heidelberg, 2010, and references cited therein.
2. Negishi, Y.; Nobusada, K.; Tsukuda, T. Glutathione-Protected Gold Clusters Revisited: Bridging the Gap between Gold(I)–Thiolate Complexes and Thiolate-Protected Gold Nanocrystals. *J. Am. Chem. Soc.* **2005**, *127*, 5261–5270.
3. Petty, J. T.; Zheng, J.; Hud, N. V.; Dickson, R. M. DNA-Templated Ag Nanocluster Formation. *J. Am. Chem. Soc.* **2004**, *126*, 5207–5212.
4. Thumu, U. B. R.; Pradeep, T. Two Luminescent Silver Clusters by Interfacial Synthesis. *Anew. Chem., Int. Ed.* **2010**, *49*, 3925–3929.
5. Thumu, U. B. R.; Boodeppa, N.; Pradeep, T. Ag_9 Quantum Cluster through a Solid State Route. *J. Am. Chem. Soc.* **2010**, *132*, 16304–16307.
6. Shibu, E. S.; Muhammed, M. A. H; Tsukuda, T.; Pradeep, T. Ligand Exchange of $Au_{25}SG_{18}$ Leading to Functionalized Gold Clusters: Spectroscopy, Kinetics, and Luminescence. *J. Phys. Chem. C* **2008**, *112*, 12168–12176.
7. Heaven, M. W.; Dass, A.; White, P. S.; Holt, K. M.; Murray, R. W. Crystal Structure of the Gold Nanoparticle $[N(C_8H_{17})_4][Au_{25}(SCH_2CH_2Ph)_{18}]$. *J. Am. Chem. Soc.* **2008**, *130*, 3754–3755.
8. Akola, J.; Walter, M.; Whetten, R. L.; Häkkinen, H.; Grönbeck, H. On the Structure of Thiolate-Protected Au_{25}. *J. Am. Chem. Soc.* **2008**, *130*, 3756–3757.
9. Dass, A. Mass Spectrometric Identification of $Au_{68}(SR)_{34}$ Molecular Gold Nanoclusters with 34-Electron Shell Closing. *J. Am. Chem. Soc.* **2009**, *131*, 11666–11667.
10. Price, R. C.; Whetten, R. L. Raman Spectroscopy of Benzenethiolates on Nanometer-Scale Gold Clusters. *J. Phys. Chem. B* **2006**, *110*, 22166–22171.
11. Dìez, I.; Pusa, M.; Kulmala, S.; Jiang, H.; Walther, A.; Goldmann, A. S.; Müller, A. H. E.; Ikkala, O.; Ras, R. H. A. Color Tunability and Electrochemiluminescence of Silver Nanoclusters. *Angew. Chem., Int. Ed.* **2009**, *48*, 2122–2125.
12. Lopez-Acevedo, O.; Tsunoyama, H.; Tsukuda, T.; Häkkinen, H.; Aikens, C. M. Chirality and Electronic Structure of the Thiolate-Protected Au_{38} Nanocluster. *J. Am. Chem. Soc.* **2010**, *132*, 8210–8218.

13. Wang, Z. W.; Toikkanen, O.; Yin, F.; Li, Z. Y.; Quinn, B. M.; Palmer, R. E. Counting the Atoms in Supported, Monolayer-Protected Gold Clusters. *J. Am. Chem. Soc.* **2010**, *132*, 2854–2855.
14. Harkness, K. M.; Cliffel, D. E.; McLean, J. A. Characterization of Thiolate-Protected Gold Nanoparticles by Mass Spectrometry. *Analyst* **2010**, *135*, 868–874.
15. Whetten, R. L.; Khoury, J. T.; Alvarez, M. M.; Murthy, S.; Vezmar, I.; Wang, Z. L.; Stephens, P. W.; Cleveland, C. L.; Luedtke, W. D.; Landman, U. Nanocrystal Gold Molecules. *Adv. Mater.* **1996**, *8*, 428–433.
16. Schaaff, T. G.; Knight, G.; Shafigullin, M. N.; Borkman, R. F.; Whetten, R. L. Isolation and Selected Properties of a 10.4 kDa Gold:Glutathione Cluster Compound. *J. Phys. Chem. B* **1998**, *102*, 10645–10646.
17. Negishi, Y.; Takasugi, Y.; Sato, S.; Yao, H.; Kimura, K.; Tsukuda, T. Magic-Numbered Au_n Clusters Protected by Glutathione Monolayers (n = 18, 21, 25, 28, 32, 39): Isolation and Spectroscopic Characterization. *J. Am. Chem. Soc.* **2004**, *126*, 6518–6519.
18. Dharmaratne, A. C.; Krick, T.; Dass, A. Nanocluster Size Evolution Studied by Mass Spectrometry in Room Temperature $Au_{25}(SR)_{18}$ Synthesis. *J. Am. Chem. Soc.* **2009**, *131*, 13604–13605.
19. Shao, N.; Huang, W.; Gao, Y.; Wang, L. M.; Li, X.; Wang, L. S.; Zeng, X. C. Probing the Structural Evolution of Medium-Sized Gold Clusters: Au_n^- (n = 27−35). *J. Am. Chem. Soc.* **2010**, *132*, 6596–6605.
20. Yao, T.; Sun, Z.; Li, Y.; Pan, Z.; Wei, H.; Xie, Y.; Nomura, M.; Niwa, Y.; Yan, W.; Wu, Z.; et al. Insights into Initial Kinetic Nucleation of Gold Nanocrystals. *J. Am. Chem. Soc.* **2010**, *132*, 7696–7701.
21. Dickerson, M. B.; Sandhage, K. H.; Naik, R. R. Protein- and Peptide-Directed Syntheses of Inorganic Materials. *Chem. Rev.* **2008**, *108*, 4935–4978 and the references cited therein.
22. Xie, J.; Zheng, Y.; Ying, J. Y. Protein-Directed Synthesis of Highly Fluorescent Gold Nanoclusters. *J. Am. Chem. Soc.* **2009**, *131*, 888–889.
23. Xavier, P. L.; Chaudhari, K.; Verma, P. K.; Pal, S. K.; Pradeep, T. Luminescent Quantum Clusters of Gold in Transferrin Family Protein, Lactoferrin Exhibiting FRET. *Nanoscale* **2010**, *2*, 2769–2776.
24. Mathew, A.; Sajanlal, P. R.; Pradeep, T. A Fifteen Atom Silver Cluster Confined in Bovine Serum Albumin. *J. Mater. Chem.* **2011**, *21*, 11205–11212.
25. Qian, Z. M.; Li, H.; Sun, H.; Ho, K. Targeted Drug Delivery *via* the Transferrin Receptor- Mediated Endocytosis Pathway. *Pharmacol. Rev.* **2002**, *54*, 561–587.
26. Sreeprasad, T. S.; Maliyekkal, S. M.; Krishnan, D.; Chaudhari, K.; Xavier, P. L.; Pradeep, T. Transparent, Luminescent, Antibacterial and Patternable Film Forming Composites of Graphene Oxide/Reduced Graphene Oxide. *ACS Appl. Mater. Interfaces* **2011**, *3*, 2643–2654.
27. Retnakumari, A.; Setua, S.; Menon, D.; Ravindran, P.; Muhammed, H.; Pradeep, T.; Nair, S.; Koyakutty, M. Molecular Receptor Specific, Non-toxic, Near-Infrared Emitting Au Cluster-Protein Nanoconjugates for Targeted Cancer Imaging. *Nanotechnology* **2010**, *21*, 055103.
28. Muhammed, M. A. H.; Verma, P. K.; Pal, S. K.; Retnakumari, A.; Koyakutty, M.; Nair, S.; Pradeep, T. Luminescent Quantum Clusters of Gold in Bulk by Albumin-Induced Core Etching of Nanoparticles: Metal Ion Sensing, Metal Enhanced Luminescence and Biolabeling. *Chem.—Eur. J.* **2010**, *16*, 10103–10112.
29. Guével, X. L.; Daum, N.; Schneider, M. Synthesis and Characterization of Human Transferrin-Stabilized Gold Nanoclusters. *Nanotechnology* **2011**, *22*, 275103.
30. Baker, E. N.; Baker, H. M. A Structural Framework for Understanding the Multifunctional Character of Lactoferrin. *Biochimie* **2009**, *91*, 3–10.
31. Heinz, H.; Farmer, B. L.; Pandey, R. B.; Slocik, J. M.; Patnaik, S. S.; Pachter, R.; Naik, R. R. Nature of Molecular Interactions of Peptides with Gold, Palladium, and Pd−Au Bimetal Surfaces in Aqueous Solution. *J. Am. Chem. Soc.* **2009**, *131*, 9704.
32. Reith, F.; Rogers, S. L.; McPhail, D. C.; Webb, D. Biomineralization of Gold: Biofilms on Bacterioform Gold. *Science* **2006**, *313*, 233–236.
33. Meldrum, F. C.; Wade, V. J.; Nimmo, D. L.; Heywood, B. R.; Mann, S. Synthesis of Inorganic Nanophase Materials in Supramolecular Protein Cages. *Nature* **1991**, *349*, 684–687.
34. Wei, H.; Wang, Z.; Zhang, J.; House, S.; Gao, Y. G.; Yang, L.; Robinson, H.; Tan, L. H.; Xing, H.; Hou, C.; *et al.* Time-Dependent, Protein-Directed Growth of Gold Nanoparticles within a Single Crystal of Lysozyme. *Nat. Nanotechnol.* **2011**, *6*, 93–97.
35. Jin, K. S.; Rho, Y.; Kim, J.; Kim, H.; Kim, I. J.; Ree, M. Synchrotron Small-Angle X-ray Scattering Studies of the Structure of Porcine Pepsin under Various pH Conditions. *J. Phys. Chem. B* **2008**, *112*, 15821–15827.
36. Wriggers, W.; Schulten, K. Protein Domain Movements: Detection of Rigid Domains and Visualization of Hinges in Comparisons of Atomic Coordinates. *Proteins: Struct., Funct., Bioinf.* **1997**, *29*, 1–14.
37. Baker, E. N.; Anderson, B. F.; Baker, H. M.; Haridas, M.; Jameson, G. B.; Norris, G. E.; Rumball, S. V.; Smith, C. A. Structure, Function and Flexibility of Human Lactoferrin. *Int. J. Biol. Macromol.* **1991**, *13*, 122–129.
38. Mead, P. E.; Tweedie, J. W. cDNA and Protein Sequence of Bovine Lactoferrin. *Nucleic Acids Res.* **1990**, *18*, 7167.
39. Guo, S.; Li, D.; Zhang, L.; Li, J.; Wang, E. Monodisperse Mesoporous Superparamagnetic Single-Crystal Magnetite Nanoparticles for Drug Delivery. *Biomaterials* **2009**, *30*, 1881–1889.
40. Kim, J.; Lee, J. E.; Lee, J.; Yu, J. H.; Kim, B. C.; An, K.; Hwang, Y.; Shin, C. H.; Park, J. G.; Kim, J.; *et al.* Magnetic Fluorescent Delivery Vehicle Using Uniform Mesoporous Silica Spheres Embedded with Monodisperse Magnetic and Semiconductor Nanocrystals. *J. Am. Chem. Soc.* **2006**, *128*, 688–689.
41. Zhu, Y.; Qian, H.; Drake, B. A.; Jin, R. Atomically Precise $Au_{25}(SR)_{18}$ Nanoparticles as Catalysts for Selective Hydrogenation of α,β-Unsaturated Ketones and Aldehydes. *Angew. Chem., Int. Ed.* **2010**, *49*, 1295–1298.
42. Stephenson, R. C.; Clarke, S. Succinimide Formation from Aspartyl and Asparaginyl Peptides as a Model for the Spontaneous Degradation of Proteins. *J. Biol. Chem.* **1989**, *264*, 6164–4170.
43. Muhammed, M. A. H.; Verma, P. K.; Pal, S. K.; Arun, R. C. K.; Paul, S.; Omkumar, R. V.; Pradeep, T. Bright, NIR Emitting Au_{23} from Au_{25}-Characterization and Applications Including Bio-labeling. *Chem.—Eur. J.* **2009**, *15*, 10110–10120.
44. Guptasarma, P. Solution-State Characteristics of the Ultraviolet A-Induced Visible Fluorescence from Proteins. *Arch. Biochem. Biophys.* **2008**, *478*, 127–129.
45. Si, S.; Mandal, T. K. Tryptophan-Based Peptides To Synthesize Gold and Silver Nanoparticles: A Mechanistic and Kinetic Study. *Chem.—Eur. J.* **2007**, *13*, 3160–3168.
46. Goswami, N.; Makhal, A.; Pal, S. K. Toward an Alternative Intrinsic Probe for Spectroscopic Characterization of a Protein. *J. Phys. Chem. B* **2010**, *114*, 15236–15243.
47. Meagher, L.; Griesser, H. J. Interactions between Adsorbed Lactoferrin Layers Measured Directly with the Atomic Force Microscope. *Colloids Surf., B* **2002**, *23*, 125–140.
48. Persson, B. A.; Lund, M.; Forsman, J.; Chatterton, D. E. W.; Akesson, T. Molecular Evidence of Stereo-specific Lactoferrin Dimers in Solution. *Biophys. Chem.* **2010**, *151*, 187–189.
49. Schmidbaur, H; Cronje, S; Djordjevic, B; Schuster, O. Understanding Gold Chemistry through Relativity. *Chem. Phys.* **2005**, *311*, 151–161.
50. Bulaj, G.; Kortemme, T.; Goldenberg, D. P. Ionization-Reactivity Relationships for Cysteine Thiols in Polypeptides. *Biochemistry* **1998**, *37*, 8965–8972.
51. Schmidbaur, H. The Aurophilicity Phenomenon: A Decade of Experimental Findings, Theoretical Concepts and Emerging Applications. *Gold Bull.* **2000**, *33*, 3–10.
52. Runeberg, N.; Schutz, M.; Werner, H. J. The Aurophilic Attraction as Interpreted by Local Correlation Methods. *J. Chem. Phys.* **1999**, *110*, 7210–7215.

53. Madhusudhan, K. T.; Singh, N. Isolation and Characterization of a Small Molecular Weight Protein of Linseed Meal. *Phytochemistry* **1985**, *24*, 2507–2509.
54. Wu, Z.; Jin, R. On the Ligand's Role in the Fluorescence of Gold Nanoclusters. *Nano Lett.* **2010**, *10*, 2568–2573.
55. Shichibu, Y.; Konishi, K. HCl-Induced Nuclearity Convergence in Diphosphine-Protected Ultrasmall Gold Clusters: A Novel Synthetic Route to "Magic-Number" Au_{13} Clusters. *Small* **2010**, *6*, 1216–1220.
56. Zheng, J.; Petty, J. T.; Dickson, R. M. High Quantum Yield Blue Emission from Water-Soluble Au_8 Nanodots. *J. Am. Chem. Soc.* **2003**, *125*, 7780–7781.
57. Wang, D.; Imae, T. Fluorescence Emission from Dendrimers and Its pH Dependence. *J. Am. Chem. Soc.* **2004**, *126*, 13204–13205.
58. Lee, W. I.; Bae, Y.; Bard, A. J. Strong Blue Photoluminescence and ECL from OH-Terminated PAMAM Dendrimers in the Absence of Gold Nanoparticles. *J. Am. Chem. Soc.* **2004**, *126*, 8358–8359.
59. Zheng, J.; Zhang, C.; Dickson, R. M. Highly Fluorescent, Water-Soluble, Size-Tunable Gold Quantum Dots. *Phys. Rev. Lett.* **2004**, *93*, 077402.
60. Zheng, J.; Petty, J. T.; Dickson, R. M. High Quantum Yield Blue Emission from Water-Soluble Au_8 Nanodots. *J. Am. Chem. Soc.* **2003**, *125*, 7780–7781.
61. Guével, X. L.; Hötzer, B.; Jung, G.; Hollemeyer, K.; Trouillet, V.; Schneider, M. Formation of Fluorescent Metal (Au, Ag) Nanoclusters Capped in Bovine Serum Albumin Followed by Fluorescence and Spectroscopy. *J. Phys. Chem. C* **2011**, *115*, 10955–10963.
62. Bao, Y.; Zhong, C.; Vu, D. M.; Temirov, J. P.; Dyer, R. B.; Martinez, J. S. Nanoparticle-Free Synthesis of Fluorescent Gold Nanoclusters at Physiological Temperature. *J. Phys. Chem. C* **2007**, *111*, 12194–12198.
63. Kawasaki, H.; Hamaguchi, K.; Osaka, I.; Arakawa, R. ph-Dependent Synthesis of Pepsin-Mediated Gold Nanoclusters with Blue Green and Red Fluorescent Emission *Adv. Funct. Mater.* **2011**, DOI: 10.1002/adfm.201100886.